1 Supplementary material

1.1 Assessment of radar algorithm and synthesis of radar data

In this section, we report results concerning the assessment of the radar algorithm used in this study as well as a description of tools and methods used for pre- and post-processing the radar data. The list of the radar images used in this study to map the flood extent is reported in Fig. S1. The naming convention for the files obtained from https://sentinel.esa.int/web/sentinel/technical-guides/sentinel-1-sar/products-algorithms/level-1-product-formatting is also reported in the figure.

[1] S1A_IW_GRDH_1SDV_20180917T233051_20180917T233116_023745_0296D5_3754
[2] S1A_IW_GRDH_1SDV_20180917T233001_20180917T233026_023745_0296D5_F6E0
[3] S1A_IW_GRDH_1SDV_20180914T230548_20180914T230617_023701_029566_B76A
[4] S1A_IW_GRDH_1SDV_20180917T233026_20180917T233051_023745_0296D5_14AD
[5] S1A_IW_GRDH_1SDV_20180919T231440_20180919T231505_023774_0297CC_D28C
[6] S1B_IW_GRDH_1SDV_20180918T232157_20180918T232222_012776_01795C_20B4
[7] S1B_IW_GRDH_1SDV_20180914T111505_20180914T111530_012710_017758_ACED
[8] S1A_IW_GRDH_1SDV_20180919T231350_20180919T231415_023774_0297CC_B86C
[9] S1B_IW_GRDH_1SDV_20180919T112319_20180919T112344_012783_017990_1394
[10] S1B_IW_GRDH_1SDV_20180919T112254_20180919T112319_012783_017990_0FA8
[11] S1B_IW_GRDH_1SDV_20180919T112344_20180919T112409_012783_017990_60F5
[12] S1B_IW_GRDH_1SDV_20180918T232107_20180918T232132_012776_01795C_28B3

Fig. S1 Naming convention and names of the Sentinel-1 files used in this study.

We pre-process Sentinel – 1 data using the Science Toolbox Exploitation Platform (SNAP) Toolkit developed by ESA (http://step.esa.int/main/toolboxes/snap/). Specifically, we first apply orbit and radiometric corrections, followed by filtering the dataset using a Lee-Sigma filter (Lee et al., 2009) with a 5 x 5 kernel to reduce speckle noise and terrain flattening and correction. Lastly, we convert backscatter intensities into a decibel-scale (dB) and export the image as a GeoTIFF with a 10 m spatial resolution.

As mentioned in the description of methods, a major issue can arise from the absence of a clear bimodality of the distribution of the recorded backscattering values, as the algorithm might not be able to select a realistic threshold for separating flooded and not-flooded regions. To mitigate this problem, following the approaches by Bovolo and Bruzzone (2007) and Martinis *et al.* (2015), we divide the SAR image in tiles. In order, to estimate an optimal number of tiles we compute the so-called Ashman coefficient (Ashman et al., 1994) defined as

$$A(h) = \sqrt{2}\frac{|\mu_1 - \mu_2|}{\sqrt{\sigma_1^2 + \sigma_2^2}} \qquad \text{(S1)}$$

where h is the specific histogram and μ1, μ2, σ1 and σ2 are, respectively, the mean (μ1 and μ2) and standard deviations (σ1 and σ2) of the two normal distributions. The higher the Ashman coefficient the more the two normal distributions are separated. For this study, we adopt a minimum value of 2 on the Ashman coefficient to ensure separability (Chini et al., 2017). For those tiles when the Ashman coefficient is below 2, we use the mean values of the coefficients surrounding that tile.

We use the data collected before Florence on 2 September, 2018 to quantify the omission and commission errors of the radar-based technique by comparing the flooded areas identified by Sentinel-1 with those present in the LULC map from the National Land Cover Database (NCLD, e.g. Jin et al., 2011; Xian et al., 2011). In Table S1, the term "Match" refers to the percentage of the areas identified as water by Sentinel-1 matching the water in the LULC dataset. "False positive" refers to the areas where Sentinel-1 suggests water but this is not the case for the LULC dataset. In the Table we report the results in the case of no erosion/dilation of the Sentinel flooded maps and when erosion and dilation (in this order) are applied with a square filter of 5 x 5, 10 x 10 and 20 x 20 pixels. The matching between Sentinel-derived and LULC water masks exceeds 99 % in many of the cases using the VH polarization with false positive values being of the order of 5 %. Overall, best results are obtained in the case of VH polarization with a erosion/dilation window of 5 pixels, showing a matching percentage greater than 99 % and the lowest false positive value. False positive values are driven not only by the overestimation of flood extent by the radar due to noise or spatial features that might mimic the electromagnetic behavior of flooded regions but also to errors in the LULC map. Figures S2 and S3 show the LULC classes (coded according to the original LANDSAT LULC product) and the Sentinel-1 backscattering coefficients (VH) over two areas within the area highlighted in the squares in Figure 1a together the water masks obtained from the LANDSAT and from the Sentinel-1 using the σ_{th2} threshold. The visual inspection of the water masks from LANDSAT indicates that LANDSAT tends to misclassify water in those areas where water bodies such as relatively narrow streams or mixed pixels occur, as highlighted, for example, by the squares in the figures. This increases our confidence in the inundated areas maps obtained from Sentinel-1 using the σ_{th2} threshold value. Therefore, we used this option to extract the pas used to detect flooded areas and merge them with those obtained from FEMA.

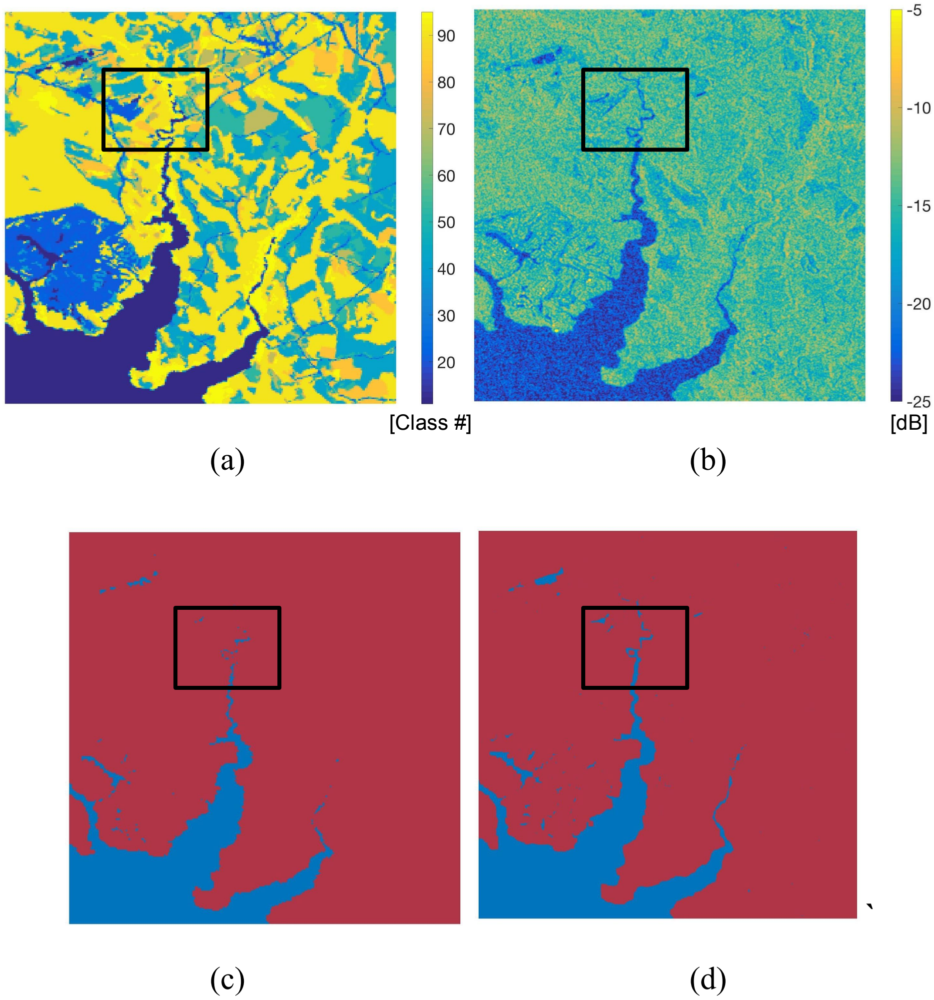

Figure S2 a) LULC map of the area contained in the rectangle A in Figure 1a. b) map of Sentinel-1 backscattering coefficient over the same region as in Figure 1. c) and d) water masks (blue indicates the presence of water) obtained from c) the LULC Landsat and d) Sentinel-1 using the σ_{Thr1} as a threshold coefficient and dilating and eroding by 10 pixels using a square filter.

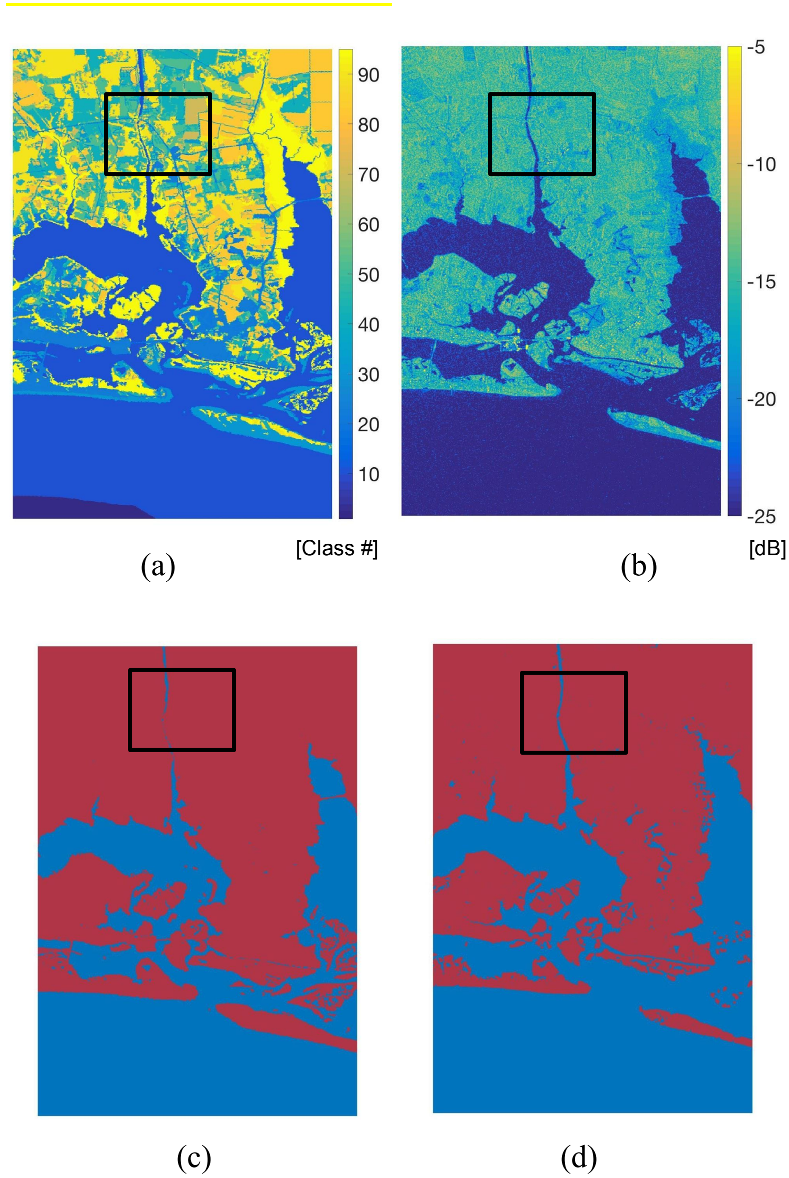

Figure S3 Same as Figure 15 but for the area B indicated in Figure 1a.

			No eros./dil.	5 x 5	10 x 10	20 x 20
VV	σ_{Thr1}	Match	97.23 %	98.34 %	98.37 %	98.24%
		False positive	5.43 %	5.22 %	6.43 %	9.60 %
	σ_{Thr2}	Match	98.11 %	99.14 %	99.30 %	99.48 %
		False positive	5.03 %	5.53 %	5.85 %	8.78 %
VH	σ_{Thr1}	Match	99.18 %	99.69 %	99.77 %	99.8 4%
		False positive	4.58 %	4.88 %	5.83 %	8.56 %
	σ_{Thr2}	Match	98.21 %	99.52 %	99.70 %	99.78 %
		False positive	4.08 %	4.33 %	4.96 %	6.86 %

Table S1 Percentage of matching and false positive between the LANDSAT-based water classification and the Sentinel-1 estimated water mask. Here, "match" refers to the case when both LANDSAT and Sentinel-1 indicate water is present. In this case, the percentage is computed using the total number of pixels classified as water by LANDSAT. "False positive" refers to the case when LANDSAT does not indicate water but Sentinel-1 does. In this case, the percentage is relative to the total number of pixels in the image minus the number of pixels classified by water in the LANDSAT dataset. No eros.dil. refers to the values obtained from the radar water masks without any dilation and/or erosion applied. The following columns indicate the values obtained when applying, in this order, dilation and erosion with a square of 5, 10 and 20 pixels, respectively.